Proceedings 10th NUMGE 2023
10th European Conference on Numerical Methods in Geotechnical Engineering
Zdravkovic L, Kontoe S, Taborda DMG, Tsiampousi A (eds)

https://doi.org/10.53243/NUMGE2023-429

Granular media modeled by flexible polyhedra using the virtual element method

P. Wriggers[1], A. Gay Neto[2], B. Hudobivnik[1], T.F. Moherdaui[2]

[1] *Institut für Kontinuumsmechanik, Leibniz Universität-Hannover, Germany*
[2] *Polytechnic School at the University of Sao Paulo, Brazil*

ABSTRACT: Granular materials, can be simulated by the discrete element method (DEM). In DEM particles are considered rigid and the only flexibility present in the model is local and formulated for the contacting points. Such treatment might not be adequate when the general flexibility of particles needs to be considered in granular media. In this contribution, we propose a method that introduces flexible particles of general polyhedral shape within the DEM context. In detail, the virtual element method (VEM) is used for the spatial discretization of particles. It allows the discretization of such polyhedra using only one single element with polyhedral shape. Contact between polyhedral particles, which can be non-convex, is addressed by a special master-to-master contact technique. Furthermore, a barrier-based interface law enforces the contact constraints. Examples include studies of systems of flexible polyhedral particles employed to model a sand-material.

Keywords: finite element; finite difference; discrete element; material point; virtual element

1 INTRODUCTION

Computational modeling allows nowadays reliable predictions of engineering problems. With the aid of simulation tools, it is possible to investigate complex systems composed of parts, joints, connections, and complex kinematics, aiming at simulating their mechanical behaviour. With virtual tests, under as tension, compression, and shear conditions, one can reduce the number of experiments. The representativity of such tests, however, depends deeply on the nature of the material behaviour related to the model.

In this context, one can assume continuum mechanics as the basis for material modeling. This comprises a myriad of models, from the linear-elastic behavior (Hooke's law), to equations that introduce more effects such as plasticity, viscoelasticity, damage, etc. An alternative methodology, particularly useful for modeling granular media, avoids the continuum mechanics assumption and represents the motion of each grain of the material individually. This possibility is very challenging from the computational perspective, as the motion of each grain is based on six equations (translations and rotations) in the three-dimensional space if one assumes rigid particles. Therefore, many grains can lead to a large set of ordinary differential equations. This approach forms the basis of the Discrete Element Method (DEM), which proposes the solution for the motion of each grain, thus, representing a coupled multibody system (see e.g.: (Poschel et al. 2005), (Cundall et al. 1979), (Luding, 2008)). A convenient geometrical representation for each grain shape is a sphere, but the real shape of granular material can better be described by polyhedra. The latter is quite general, as one can describe convex or concave grains, including details of the boundaries.

The main difficulty of DEM relates to the modelling of grain-grain interaction. For that, one can establish proper interface laws, that characterize the complexity of each local contact patch. As examples, one can formulate a simple linear (spring-type) interface law or a Hertzian-like relation between normal force and grain-grain approach (Johnson, 1987). DEM models, however, assume each grain as a rigid body. Therefore, flexibility is usually only embedded in the interface law, representing very local effects. This can be an issue when the overall system flexibility is of interest. A remedy for this limitation is a solid modelling for each grain. With that, each grain can be approximated using techniques such as the finite element method (FEM). For complex grain shapes, the FEM discretization leads to grains with many elements and unknowns. This turns out to be computationally demanding and leads to an overall DEM-FEM model that is even more complex and for practical applications impossible to be solved. The virtual element method (VEM) provides an alternative to FEM and has a more versatile option to complex element shapes, enabling to use just one element to describe a polyhedron.

Polyhedral representation of grains is a possible choice when using DEM models, see e.g. [(Benjamin et al. 2013), (Bart et al. 2015), (Fei et al. 2018), (Gay Neto

et al. 2022)]. With such geometrical description, theoretically any grain shape, convex/concave, can be modeled with a desired level of geometrical refinement. However, contact detection between general polyhedra is challenging and costly. Due to that, spheres are the most popular choice for particle shapes in DEM. When aiming at a more accurate representation of particle shapes, spheres are no longer acceptable and one needs another option, facing higher computational costs (such as polyhedra or sphere clusters).

The polyhedral representation for each grain can be incorporated via VEM in a DEM code when the particle flexibility is of concern. Here we introduce a single element per grain scheme, see Figure 1. This significantly simplifies the meshing process and proposes a simple, but powerful formulation to include a grain flexibility. It can be shown that even a single virtual element is capable to capture grain elasticity. This so called VEM-DEM scheme was proposed in (Gay Neto et al., 2021).

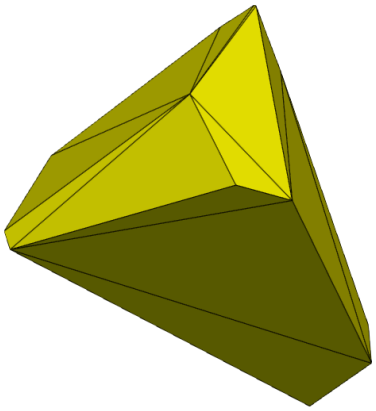

Figure 1. VEM-DEM scheme: a single grain is represented as a single flexible polyhedral element

This paper illustrates the basic ideas of the VEM-DEM scheme, and its usage for a numerical simulation of sand material. At this stage results are only for a limited amount of but next developments will result in a code that can be applied in engineering practice.

2 BRIEF DESCRIPTION OF VEM-DEM SCHEME

To formulate of the general motion of a grain we introduce the total potential W which is split onto an internal part, related to the strain energy W_i in the grain, and external part W_e, related to the loading, and a part that contains the inertia terms, W_d.

$$\boldsymbol{W = W_i - W_e + W_d}. \qquad (1)$$

The strain energy that is used in this contribution relates to a nonlinear Neo-Hookean hyperelastic model ψ_i

$$\boldsymbol{\psi_i(F) = \frac{\mu}{2}\left(J_F^{-\frac{3}{2}} tr(F^T F) - 3\right) + \frac{\kappa}{4}\left(J_F^2 - 1 - 2\log(J_F)\right)}. \qquad (2)$$

which is a function of the deformation gradient $\boldsymbol{F}$ and its determinant J_F. The parameters κ and μ are the bulk and the shear modulus, respectively. The deformation gradient follows from $\boldsymbol{F = 1 + Grad\, u}$.

2.1 Virtual element method (VEM)

The virtual element method is a generalization of the finite element method that allows for elements with arbitrary shape and polynomial order. Its basic principles were first published in (Beirão da Veiga et al. 2013), a more practical introduction to the method can be found in (Beirão da Veiga et al. 2014). Some examples regarding applications in solid mechanics can be found in (Hudobivnik et al. 2019), (Park et al. 2020), (Cihan et al. 2021), (Cihan et al. 2022). The method's solution space contains non-polynomial functions in addition to a full polynomial subspace of the used polynomial order k. Within the method the field of displacements $\boldsymbol{u(X}, t)$ is approximated only at the edges of each particle.

A linear interpolation, degree $k = 1$, is employed for simplicity and efficiency in this contribution. A more detailed explanation can be found in (Gay Neto et al., 2021) for the method used in this work.

2.1.1 VEM construction

Let $\boldsymbol{p_E}$ be the chosen degrees of freedom (DOF) for the element E. Let us further assume that n_E elements descibe the system of particles. The potential W is then described using the contribution of all n_E elements, each element contribution is given by $W_E(\boldsymbol{p_E})$, which can be decomposed into internal $W_{E\,i}(\boldsymbol{p_E})$, external $W_{E\,e}(\boldsymbol{p_E})$ and inertial $W_{E\,d}(\boldsymbol{p_E})$ parts.

The VEM ansatz for the displacements $\boldsymbol{u_h}$ is unknown within the element, it is only defined at the edges. It's projection onto the polynomial subspace $\boldsymbol{u_\Pi}$ can be constructed, leading to a split of the element's contribution to the potential into two parts. The first part is a function of $\boldsymbol{u_\Pi}$, which alone yields rank deficient stiffness and mass matrices. It is called consistency part W_E^{con}. The second part relates to the stability term W_E^{sta}, needed to restore the rank of the formulation.

$$\mathbf{W_E}(\boldsymbol{p_E}) = \boldsymbol{W_E^{con}(u_\Pi) + W_E^{sta}(u_h - u_\Pi)}. \qquad (3)$$

2.1.2 Virtual element ansatz and projection

The polynomial projection of the ansatz functions is defined by the orthogonality conditons (4) and (5) which

have to be satisfied for all displacements $\boldsymbol{u_p} \in \left(P_k(\Omega)\right)^3$ of the polynomial interpolation space with order k

$$\int_{\Omega}\left[\boldsymbol{u_p} \cdot (\boldsymbol{u_h} - \boldsymbol{u_\Pi})\right] d\boldsymbol{\Omega} = \mathbf{0}. \quad (4)$$

$$\int_{\Omega}\left[\boldsymbol{\nabla u_p} \cdot (\boldsymbol{\nabla u_h} - \boldsymbol{\nabla u_\Pi})\right] d\boldsymbol{\Omega} = \mathbf{0}. \quad (5)$$

Condition (5) can be reformulated with the divergence theorem. This yields after some algebra the gradient of the projection as presented in (6). Furthermore, condition (4), for $k = 1$, can be used to compute the constant part of $\boldsymbol{u_\Pi}$. The integral in (4) can be replaced by the nodal average of the displacements. The right side of expression in (6) can be computed using a triangulation of each of the faces $\partial\Omega_f$ of the polyhedron with $\partial\Omega = \sum_f \partial\Omega_f$, requiring knowledge of the vertex displacements, i.e., $\boldsymbol{u_\Pi} = \boldsymbol{u_\Pi}(\boldsymbol{p_E})$.

$$\boldsymbol{\nabla u_\Pi}|\boldsymbol{\Omega}| = \int_{\Omega} \boldsymbol{\nabla u_h}\, d\boldsymbol{\Omega} = \int_{\partial\Omega} \boldsymbol{u_h} \otimes \boldsymbol{N}\, d\boldsymbol{A}. \quad (6)$$

2.1.3 Consistency term

The polynomial part of the element's contribution to the problem's potential $W_E^{con}(\boldsymbol{u_\Pi})$ can easily be computed using quadrature schemes as only polynomials are used for the interpolation.

2.1.4 Stabilization

The consistency part alone yields a rank deficient stiffness and mass matrices, thus, a stabilization term is needed.

In this work the sub-mesh approach is employed to stabilize the element, see (Hudobivnik et al. 2019). Here, an additional energy term is introduced, based on a tetrahedral sub-mesh of finite elements $W_E(\boldsymbol{u_h})$, valid for all components of the potential ($x = i, e, d$). In this case, $W_{Ex}(\boldsymbol{u_\Pi})$ is the x part of consistency term.

$$\boldsymbol{W_{Ex}^{sta}} = \boldsymbol{\beta_x W_{Ex}}(\boldsymbol{u_h}) - \boldsymbol{\beta_x W_{Ex}}(\boldsymbol{u_\Pi}). \quad (7)$$

2.1.5 Full potential

The full potential of an element E can be expressed like (3), with each component being defined as

$$\begin{aligned} \boldsymbol{W_{E\,i}}(\boldsymbol{p_E}) &= (\mathbf{1} - \boldsymbol{\beta_i})\boldsymbol{W_{E\,i}}(\boldsymbol{u_\Pi}) + \boldsymbol{\beta_i W_{E\,i}}(\boldsymbol{u_h}) \\ \boldsymbol{W_{E\,e}}(\boldsymbol{p_E}) &= (\mathbf{1} - \boldsymbol{\beta_e})\boldsymbol{W_{E\,e}}(\boldsymbol{u_\Pi}) + \boldsymbol{\beta_e W_{E\,e}}(\boldsymbol{u_h}). \\ \boldsymbol{W_{E\,d}}(\boldsymbol{p_E}) &= (\mathbf{1} - \boldsymbol{\beta_d})\boldsymbol{W_{E\,d}}(\boldsymbol{u_\Pi}) + \boldsymbol{\beta_d W_{E\,d}}(\boldsymbol{u_h}) \end{aligned} \quad (8)$$

Each element's contribution to the residual and tangent matrices can be computed as usual based on the potential just presented, see (Gay Neto et al., 2021).

This virtual element formulation was applied to single virtual elements of different shape. For a compressive loading the force versus strain curves were compared with refined finite element discretizations of the same particle, see (Gay Neto et al., 2021). Remarkedly, the single VEM element performed well for situations up to 20 % strain besides having only constant stress states inside due to the linear interpolation.

2.2 Master-to-master contact method

Pointwise contact interactions between general surfaces can be established by a master-to-master contact scheme, see (Gay Neto et al. 2016). In this approach, two surfaces $\Gamma_A(\zeta_A, \theta_A)$ and $\Gamma_B(\zeta_B, \theta_B)$ are defined in terms of convective coordinates. These define a vector gap

$$\mathbf{g} = \boldsymbol{\Gamma_A}(\boldsymbol{\zeta_A}, \boldsymbol{\theta_A}) - \boldsymbol{\Gamma_B}(\boldsymbol{\zeta_B}, \boldsymbol{\theta_B}). \quad (9)$$

The magnitude $\|\mathbf{g}\|$ is a distance measure. The direction of $\mathbf{g}$ can be used to define the contact "normal"

$$\mathbf{n} = \frac{\mathbf{g}}{\|\mathbf{g}\|}. \quad (10)$$

The gap can be evaluated by picking arbitrary material points in both surfaces. Then, one needs to establish a methodology to determine the contact pairs. This is done by the so-called Local Contact Problem (LCP), leading to the orthogonality relations

$$\begin{cases} +\boldsymbol{\Gamma_{A,\zeta_A}} \cdot \mathbf{g} \\ +\boldsymbol{\Gamma_{A,\theta_A}} \cdot \mathbf{g} \\ -\boldsymbol{\Gamma_{B,\zeta_B}} \cdot \mathbf{g} \\ -\boldsymbol{\Gamma_{B,\theta_B}} \cdot \mathbf{g} \end{cases} = \begin{bmatrix} \mathbf{0} \\ \mathbf{0} \\ \mathbf{0} \\ \mathbf{0} \end{bmatrix}. \quad (11)$$

The solution of this nonlinear set of equations leads to parameters associated with the positions of material points $[\bar{\zeta}_A \quad \bar{\theta}_A \quad \bar{\zeta}_B \quad \bar{\theta}_B]$ where contact takes place. All ingredients used in this method are geometrical. Due to that, one can adapt the original definition of a LCP which degenerates the contacting surfaces into curves or points. By adapting the LCP definition, the contact interaction of edge-to-edge, vertex-to-face, vertex-to-edge, or vertex-to-vertex can be found, see (Gay Neto et al. 2019). This leads to the proposal in (Gay Neto et al. 2021) to address general contact between polyhedra, where all combinations of such contact possibilities are considered.

3 SIMULATIONS AND RESULTS

Numerical simulations are presented to show that the proposed technique can be used to address granular media. We construct a sand-like granular material pack specimen by filling it into a box with rigid walls. It is formed by employing 515 polyhedral particles (with size approx. 1.45 mm), which are inserted inside a box of dimensions 8 mm x 8 mm. The pack has a height of approx. 6 mm, see *Figure 2*. The Young modulus is E = 90 GPa, the Poisson ratio is $\nu = 0.16$ and the specific mass is 2,200 kg/m^3. Note that the bulk and the shear modulus can be easily obtained form Young`s modulus and Poisson ratio.

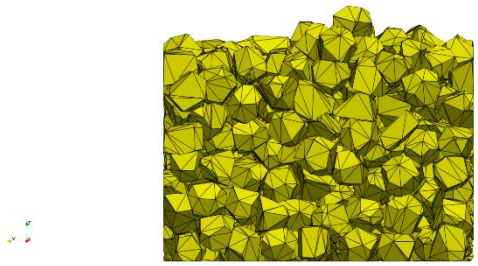

Figure 2. Sand-like granular material pack (initial configuration)

The granular material is released by taking away the vertical walls. Then for three different friction coefficients we observe in Fig.3, Fig. 4 and Fig. 5 the final configuration of the sand pile. Clearly the slope angle reduces for smaller friction coefficients.

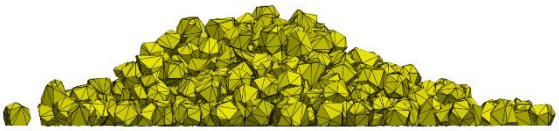

Figure 3. Sand-like granular material pack dismounting simulation – static friction 0.9, dynamic friction 0.8

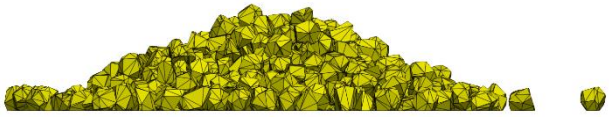

Figure 4. Sand-like granular material pack dismounting simulation – static friction 0.6, dynamic friction 0.5

Figure 5. Sand-like granular material pack dismounting simulation – static friction 0.3, dynamic friction 0.2

The next simulation is related to a compression test where granular material in a box, see Fig. 6, is compressed by a certain vertical pressure. The same material parameters as in the first example are used. Only the friction coefficient is changed, see Fig. 6.

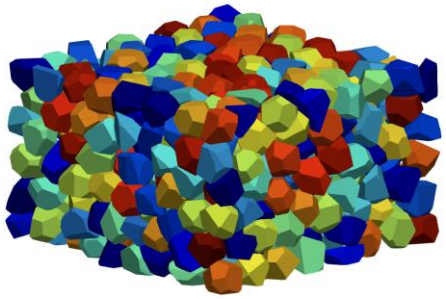

Figure 6. Sand-like granular material pack (compressed configuration) – static friction 0.15, dynamic friction 0.15

The pack is compressed by a "lid" surface, located above the pack. The vertical motion of the lid ranges from 7 mm to 4,9 mm within the loading and unloading phase. This loading yields the response curve depicted in Fig. 7 where the difference between loading and unloading curve shows the internal friction within the compressed granular material.

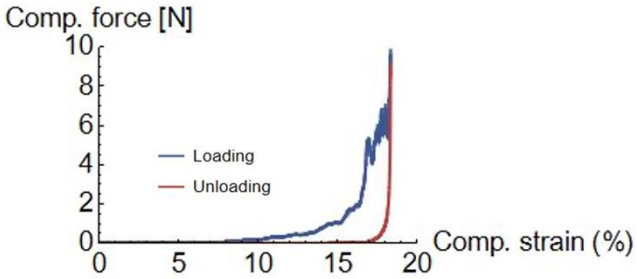

Figure 7. Sand-like granular material pack. Compression force vs. compressive strain for loading and unloading phases of the simulation

4 CONCLUSIONS

A novel methodology was developed to simulate systems composed of flexible polyhedral particles that can undergo multiple contact interactions. These particles were modeled using the virtual element method which allows to discretize polyhedral grains with single elements. In the numerical simulations it was shown that the constitutive behaviour of stiff particle assemblies under compression could be captured, including the hysteresis curve.

5 ACKNOWLEDGEMENTS

The first author acknowledges funding by the Deutsche Forschungsgemeinschaft (DFG, German Research Foundation) under Germany's Excellence Strategy within the Cluster of Excellence PhoenixD, EXC 2122 (project number: 390833453). The second author acknowledges CNPq for the research grant 304321/2021-4.

6 REFERENCES

Beirão da Veiga, L., Brezzi, F., Cangiani, A., Manzini, G., Marini, L. D., & Russo, A. 2013. Basic Principles of Virtual Element Methods. *Mathematical Models and Methods in Applied Sciences*, *23*(01), 199–214. https://doi.org/10.1142/S0218202512500492

Beirão da Veiga, L., Brezzi, F., Marini, L. D., & Russo, A. 2014. The Hitchhiker's Guide to the Virtual Element Method. *Mathematical Models and Methods in Applied Sciences*, *24*(08), 1541–1573. https://doi.org/10.1142/S021820251440003X

Cihan, M., Hudobivnik, B., Aldakheel, F., & Wriggers, P. 2021. Virtual Element Formulation for Finite Strain Elastodynamics. *Computer Modeling in Engineering & Sciences*, *129*(3), 1151–1180. https://doi.org/10.32604/cmes.2021.016851

Cihan, M., Hudobivnik, B., Korelc, J., & Wriggers, P. 2022. A virtual element method for 3D contact problems with non-conforming meshes. *Computer Methods in Applied Mechanics and Engineering*, *402*, 115385. https://doi.org/10.1016/j.cma.2022.115385

Cundall, P. A., & Strack, O. D. L. 1979. A discrete numerical model for granular assemblies. *Géotechnique*, *29*(1), 47–65. https://doi.org/10.1680/geot.1979.29.1.47

Gay Neto, A., Hudobivnik, B., Moherdaui, T. F., & Wriggers, P. 2021. Flexible polyhedra modeled by the virtual element method in a discrete element context. *Computer Methods in Applied Mechanics and Engineering*, *387*. https://doi.org/10.1016/j.cma.2021.114163

Gay Neto, A., Pimenta, P. M., & Wriggers, P. 2016. A master-surface to master-surface formulation for beam to beam contact. Part I: frictionless interaction. *Computer Methods in Applied Mechanics and Engineering*, *303*, 400–429. https://doi.org/10.1016/j.cma.2016.02.005

Hudobivnik, B., Aldakheel, F., & Wriggers, P. 2019. A low order 3D virtual element formulation for finite elasto–plastic deformations. *Computational Mechanics*, *63*(2), 253–269. https://doi.org/10.1007/s00466-018-1593-6

Johnson, K. L. 1985. Contact Mechanics. In *Handbook of Lubrication and Tribology, Volume II: Theory and Design, Second Edition*. Cambridge University Press. https://doi.org/10.1017/CBO9781139171731

Luding, S. 2008. Introduction to discrete element methods. *European Journal of Environmental and Civil Engineering*, *12*(7–8), 785–826. https://doi.org/10.1080/19648189.2008.9693050

Nassauer, B., Liedke, T., & Kuna, M. 2013. Polyhedral particles for the discrete element method. *Granular Matter*, *15*(1), 85–93. https://doi.org/10.1007/s10035-012-0381-9

Neto, A. G., & Wriggers, P. 2022. Discrete element model for general polyhedra. *Computational Particle Mechanics*, *9*(2), 353–380. https://doi.org/10.1007/s40571-021-00415-z

Park, K., Chi, H., & Paulino, G. H. 2020. Numerical recipes for elastodynamic virtual element methods with explicit time integration. *International Journal for Numerical Methods in Engineering*, *121*(1), 1–31. https://doi.org/10.1002/nme.6173

Pöschel, T., & Schwager, T. 2005. *Computational Granular Dynamics* (1st ed.). Springer-Verlag. https://doi.org/10.1007/3-540-27720-X

Smeets, B., Odenthal, T., Vanmaercke, S., & Ramon, H. 2015. Polygon-based contact description for modeling arbitrary polyhedra in the Discrete Element Method. *Computer Methods in Applied Mechanics and Engineering*, *290*, 277–289. https://doi.org/10.1016/j.cma.2015.03.004

Zheng, F., Jiao, Y.-Y., & Sitar, N. 2018. Generalized contact model for polyhedra in three-dimensional discontinuous deformation analysis. *International Journal for Numerical and Analytical Methods in Geomechanics*, *42*(13), 1471–1492. https://doi.org/10.1002/nag.2798